

## RESEARCH ARTICLE

# Seashell-based bioceramics for advanced electrospun tissue scaffolds

Sema Nur Sahin<sup>1,2</sup>  | Erdi Bulus<sup>1,3</sup>  | Alper Tezcan<sup>1,4</sup>  | Muhammad Umar Farooq<sup>5</sup>   
Marwah Al-garash<sup>2</sup>  | Yesim Muge Sahin<sup>1,2\*</sup> 

<sup>1</sup> Istanbul Arel University, ArelPOTKAM (Polymer Technologies and Composite Application and Research Center), Istanbul, Türkiye  
ROR ID: [03natay60](https://ror.org/03natay60)

<sup>2</sup> Istanbul Arel University, Biomedical Engineering Department, Istanbul, Türkiye  
ROR ID: [03natay60](https://ror.org/03natay60)

<sup>3</sup> Istanbul Arel University, Transportation Services Civil Aviation Cabin Services Program, Vocational School, Istanbul, Türkiye  
ROR ID: [03natay60](https://ror.org/03natay60)

<sup>4</sup> Istanbul Arel University, Mechanical Engineering Department, Istanbul, Türkiye  
ROR ID: [03natay60](https://ror.org/03natay60)

<sup>5</sup> East China University of Science and Technology, State Key Laboratory of Chemical Engineering, Shanghai, China  
ROR ID: [01vyrm377](https://ror.org/01vyrm377)

\* **Corresponding author:** E-mail: [ymugesahin@arel.edu.tr](mailto:ymugesahin@arel.edu.tr); Ph.: +90 5379757507

**Citation:** Sahin, S.N., Bulus, E., Tezcan, A., Farooq, M.U., Al-garash, M., & Sahin, Y.M. (2025). Seashell-based bioceramics for advanced electrospun tissue scaffolds. *The European chemistry and biotechnology journal*, 4, 01-13.  
<https://doi.org/10.62063/ecb-49>

**License:** This article is licensed under a Creative Commons Attribution-NonCommercial 4.0 International License (CC BY-NC 4.0).

**Peer review:** Double Blind Refereeing.

**Received:** 05.01.2025

**Accepted:** 01.03.2025

**Online first:** 15.03.2025

**Published:** XX.07.2025

## Abstract

The demand for tissue scaffolds to support the repair, regeneration, and restoration of damaged tissues is rapidly growing. Scaffolds fabricated using the electrospinning technique are particularly significant in tissue engineering due to their ability to provide micro- to nano-scale porosity and a large surface area. This study focuses on developing tissue scaffolds with enhanced cell adhesion, biodegradability, and tensile strength by employing aqueous solutions of polyvinyl alcohol (PVA), a biocompatible and biodegradable synthetic polymer; gelatin (GEL), a natural polymer that offers binding sites conducive to cell adhesion and differentiation; and synthesized bioceramics, all integrated through the electrospinning process. Composite tissue scaffolds were engineered by incorporating 1% to 3% GEL into the PVA solution, followed by the addition of 1% bioceramics to the 1% GEL-enriched PVA. The composite formulation not only emulates the extracellular matrix as a biomimetic strategy but also goes beyond merely enhancing ossification. Comprehensive structural, morphological, mechanical, and thermal characterizations were conducted to analyze the properties of the scaffolds containing the synthesized bioceramics. The tensile strengths of the fabricated nanocomposites were determined to be 6.25 MPa for 10:0 (PVA:GEL), 7.45 MPa for 10:1 (PVA:GEL), 8.01 MPa for 10:3 (PVA:GEL), and 8.22 MPa for 10:1:1 (PVA:GEL:Bioceramics), respectively, indicating a progressive enhancement in mechanical properties with the incorporation of GEL and bioceramics. The results demonstrate the successful production of a potential biomaterial with ideal properties for



tissue engineering applications. These composite scaffolds, providing a conducive environment for cell adhesion and exhibiting excellent mechanical properties, are anticipated to be suitable for dental applications as an intermediate layer which may support bone and connective tissue formation.

**Keywords:** Bioceramic, tissue scaffold, electrospinning, gelatin, polyvinyl alcohol.

## Introduction

Tissue engineering is based on three key factors: cells, growth factors, and tissue scaffolds, and it is a discipline aimed at functionally restoring damaged tissues. Tissue scaffolds are regenerative structures that support tissue repair and are significant as they are used in the healing of damaged tissues and organs. They support cells when seeded *in vitro* and promote matrix formation, laying the foundation for tissue transplantation (Howard et al., 2008).

The materials used in the production of tissue scaffolds play a crucial role in promoting cell proliferation and differentiation. An ideal tissue scaffold should possess good biocompatibility, appropriate pore size and porosity, and excellent mechanical strength, while also exhibiting characteristics suitable for the specific area of the body where it will be applied (Keçeciler et al., 2023). Tissue scaffolds fabricated via the electrospinning technique have garnered significant attention in tissue engineering due to their excellent biocompatibility, optimal biodegradability, non-toxic nature, micro-to nano-scale porosity, and their ability to achieve a high surface-to-volume ratio (Sadeghi et al., 2018; Cam et al., 2019). Tissue engineering has garnered significant attention in recent years (Aydogdu et al., 2019). Polymer/ceramic composite biomaterials and tissue scaffolds produced using the electrospinning technique exhibit enhanced mechanical strength and optimal cell adhesion. The superior performance of composite materials has led to a surge in research focusing on polymer and ceramic materials (Hoque et al., 2014).

Polymer materials provide a suitable framework for replicating the natural architecture of soft tissues. Integrating bioceramics into polymers enhances their potential for repair and regeneration strategies (Zou et al., 2018; Filippi et al., 2020; Jazayeri et al., 2020). PVA, a synthetic polymer, is both biocompatible and biodegradable; however, its limited cell recognition sites reduce its bioactivity. In contrast, GEL offers numerous integrin binding sites, facilitating cell adhesion and differentiation (Heydary et al., 2015; Perez-Puyana et al., 2018). Bioceramics are widely favored for incorporation into tissue scaffolds due to their ability to support cell growth and proliferation, exhibit antimicrobial properties, contribute to the repair of bone and dental tissues, and serve as effective materials for soft tissue healing applications (Xie et al., 2019; Zhang et al., 2021). Chemical precipitation, the most commonly used technique for bioceramic synthesis, enables the production of bioceramics with high efficiency and low cost in the absence of organic solvents. Moreover, the only by-product of the reaction is water, which does not contain any other elements, making this method quite suitable for biomedical applications (Mazumder et al., 2019; Santhosh et al., 2013; Gunduz et al., 2013; Şahin et al., 2018).

In the present study, it is aimed to produce a composite tissue scaffold that mimics the extracellular matrix (ECM). For this scaffold, which was fabricated using both ECM composite components and nanoscale production, the following steps were carried out: synthesizing bioceramics from sea snail shells via chemical precipitation, incorporating the synthesized bioceramics into a PVA/gelatin (GEL) solution, and producing tissue scaffolds with suitable cell adhesion and biocompatibility via electrospinning technique. Additionally, the structural, morphological, mechanical, and thermal

characterizations of the synthesized bioceramics and the fabricated tissue scaffolds were performed to evaluate their properties for tissue engineering applications.

## Materials and methods

### Materials

For the synthesis of bioceramics, marine snail shells were obtained from a seafood company in Eminönü, Istanbul. For tissue scaffold production, a polyvinyl alcohol (PVA) polymer with a molecular weight of 85.000-124.000 g/mol was purchased from Sigma-Aldrich (Turkey). Food-grade gelatin (GEL) was acquired from a local herbalist in Eminönü, Istanbul. Ultrapure water with a resistance of 18.3 M $\Omega$  was used as the solvent for preparing the polymer solution.

### Bioceramics synthesis

Marine snail shells were selected as the source for bioceramic synthesis. Initially, the shells were sterilized in an ultrasonic bath at 90°C for 30 minutes, followed by drying in an oven at 100°C for 3 hours to ensure purification. The dried shells were then ground into powder using a ceramic mortar and further sieved through a stainless steel mesh with a size of 100  $\mu$ m to achieve a uniform particle size.

Thermal analysis was conducted to quantify the calcium carbonate (CaCO<sub>3</sub>) content in the powders. Using this data, the required amount of phosphoric acid (H<sub>3</sub>PO<sub>4</sub>) was calculated based on the stoichiometric (molar) calcium-to-phosphorus (Ca/P) ratios: 1.67 for hydroxyapatite and 1.50 for tricalcium phosphate. For each batch, 2 g of powdered shell was measured and transferred into a beaker containing 50 ml of pure water. The mixture was heated to 90°C on a magnetic stirrer, and the calculated H<sub>3</sub>PO<sub>4</sub> solution was added dropwise. Once bubbling ceased, the mixture was continuously stirred at 90°C for 8 hours and then allowed to cool to room temperature to complete the reaction. The resulting precipitate was separated by centrifugation, and the wet powder was dried in an oven at 100°C for 24 hours. The dried precipitate was sintered at 850°C for 4 hours to obtain the final bioceramic product (Sahin et al., 2018; Yelten and Yılmaz, 2010).

### Preparation of solutions

To produce composite tissue scaffolds, PVA, GEL, and bioceramic powders were dissolved in distilled water using a magnetic stirrer. A pure 10:0 (PVA: GEL) solution was prepared by dissolving 10 g of PVA in 100 ml w/v of distilled water and stirring at 80°C for 150 minutes. Subsequently, GEL was added to the 10:0 (PVA: GEL) solution in weight ratios of 1% and 3% w/v. These mixtures were stirred at 40°C for 150 and 180 minutes, respectively, to obtain 10:1 (PVA: GEL) and 10:3 (PVA: GEL) solutions (Linh et al., 2010). Finally, 1% bioceramic powder was added to the 10:1 (PVA: GEL) solution and stirred at 37°C for 210 minutes, resulting in the 10:1:1 (PVA:GEL:Bioceramics) solution (Song et al., 2010; Ba Linh et al., 2013). The preparation parameters for the solutions required for composite tissue scaffold fabrication are shown in Table 1.

**Table 1.** Preparation parameters of solutions used for the fabrication of composite tissue scaffolds.

Polymer weight ratio	Temperature (°C)	Time (min)
10:0 (PVA: GEL)	80	150
10:1 (PVA: GEL)	40	150
10:3 (PVA: GEL)	40	180
10:1:1(PVA:GEL:Bioceramics)	37	210

### 1.1. Production of composite tissue scaffolds

Composite tissue scaffolds were fabricated using the electrospinning technique by applying the working parameters listed in Table 2 (Sengor et al., 2018). To remove any residual solvents, the produced tissue scaffolds were dried in an oven at 45°C for 24 hours.

**Table 2.** Electrospinning production parameters for composite tissue scaffolds.

Polymer Content	Flow Rate (ml/hr)	Distance (cm)	Voltage (kV)
10:0 (PVA: GEL)	5.0	15	30
10:1 (PVA: GEL)	5.0	15	30
10:3 (PVA: GEL)	5.0	10	25
10:1:1(PVA: GEL:Bioceramics)	3.0	5	25

### 1.2. Characterization studies

**Fourier transform infrared (FTIR) analysis:** The presence of functional groups in the bioceramics and composite tissue scaffolds was determined by FTIR spectroscopy (FT/IR-6600, JASCO, Tokyo, Japan) in the wavelength range of 400-4400  $\text{cm}^{-1}$ . These analyzes enabled the structural characterization of the bioceramics and composites, confirming their composition and the successful incorporation of bioceramics into the composite tissue scaffolds.

**Field emission gun scanning electron microscopy (FEGSEM) analysis:** Bioceramics and composite tissue scaffolds were coated with gold-palladium under Argon (Ar) gas and analyzed using a field emission gun scanning electron microscope (FEGSEM 450, FEI Quanta, Oregon, USA). Images were captured under high vacuum at a range of 12.00-15.00 kV potential, with scales from 100-500 nm to 500 nm-2  $\mu\text{m}$ . The diameters of 40 nanofibers were measured from the images, their arithmetic mean was calculated, and the nanofiber diameter distributions were determined. For all the samples, morphological analysis was conducted at various magnifications.

**Tensile test:** The tensile test for composite tissue scaffolds was performed according to ASTM D882-10 standards using a tensile testing machine (DVT UZM K3, DVT DEVOTRANS, Istanbul, Türkiye). The test was conducted under a 500 N load, with a tensile speed of 5 mm/min.

**Thermogravimetric analysis (TGA):** The  $\text{CaCO}_3$  content of marine snail shells was determined using a TGA device (STA7200, Hitachi, Tokyo, Japan). Thermal characterization of the samples was conducted under Nitrogen ( $\text{N}_2$ ) atmosphere at a heating rate of 15°C /minute, within the temperature range of 30-900°C.

## Results and discussion

### Thermal characterization of bioceramics with TGA

Upon analysis of the TGA thermogram of sea snail shells (Figure 1), it was observed that 45.0% of the material was lost during heating, attributed to the decomposition of organic matter and impurities, while the remaining 55.0% was identified as inorganic CaO.

Using the 55.0% CaO content, the stoichiometric molar ratio corresponding to the mineral

composition of bone in the human body was calculated to determine the required amount of  $H_3PO_4$ . This calculated  $H_3PO_4$  quantity was subsequently incorporated into the CaO structure during the chemical precipitation process, enabling the successful synthesis of bioceramics.

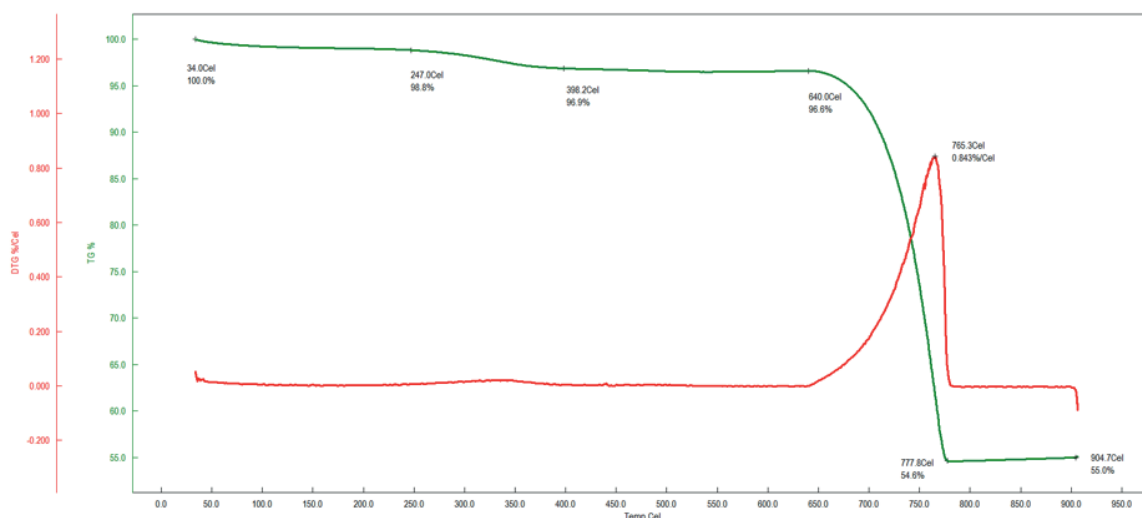


| **Figure 1.** TGA thermogram of sea snail shells.

### **Structural characterization (FTIR analysis)**

The FTIR spectra of the bioceramics and tissue scaffolds are presented in Figure 2. In the analysis of the spectra, the functional groups of the bioceramic powders sintered at 850°C for 4 hours were confirmed.

A phosphate group O–P–O bending mode was observed at 494, 528, 560, 609, 667  $cm^{-1}$  and another bending band is detected at 471  $cm^{-1}$  P–O asymmetric stretching mode bands of the phosphate group were at 973, 1031, 1066, 1101, 1139, 1187, 1211  $cm^{-1}$ . P–O–P symmetric stretching bands were obtained as medium intensity peaks at 726, 751  $cm^{-1}$ . Similarly, the phosphate group P–O symmetric stretching vibration band at 954  $cm^{-1}$  and harmonic overtone were detected at 1156  $cm^{-1}$ . These findings can be attributed to the phosphate group that consists of the hydroxyapatite formulation of the synthesized bioceramic. On the other hand, the carbonate group function was also confirmed for the bioceramic with the following findings; a carbonate group stretching mode at 1415  $cm^{-1}$  and a carbonate group bending mode at 1456  $cm^{-1}$ . The characteristic peaks of PVA, the matrix of the composite, in the membrane were also observed. Hydroxyl (–OH) groups were indicated at 3272.61  $cm^{-1}$ , and the alkyl group bands were observed at 2854.13  $cm^{-1}$  for (–CH<sub>3</sub>), 2916.81  $cm^{-1}$  for (–CH<sub>2</sub>) functional groups. The peak at 835.02  $cm^{-1}$  is due to the (–C–C–) vibrations. A weak peak at 1700–1750  $cm^{-1}$ , corresponding to the C=O (carbonyl group), can be due to residual acetic acid ester groups in PVA. The peak at 1718.26  $cm^{-1}$  can be attributed to the hydrogen bonding between the carbonyl and hydroxyl groups in PVA chains, which occurs due to hydrophilic interactions (Hernández et al., 2024; Tüzün, 2023).

These bands can vary depending on the interactions of the composite parts. For example, the –OH vibration band of PVA was detected at 3272.61  $cm^{-1}$ . When 1% GEL was added to a 10% PVA solution, no specific GEL peak was observed; however, the position of the PVA peaks shifted, and

their intensity increased. When examining the spectra of PVA and GEL, the  $-OH$  hydroxyl group at  $3272.61\text{ cm}^{-1}$  was found in the same position for both polymers, which explains the superposition of the peaks. Nonetheless, the dominant effect of GEL on PVA caused the displacement of PVA peaks. This result confirms the successful formation of a composite material as explained in the similar studies in the literature (Bulus et al., 2020; Razzaq et al., 2021). The distinctive peaks of the functional groups of PVA, Gel and bioceramic materials are shown in Figure 2.

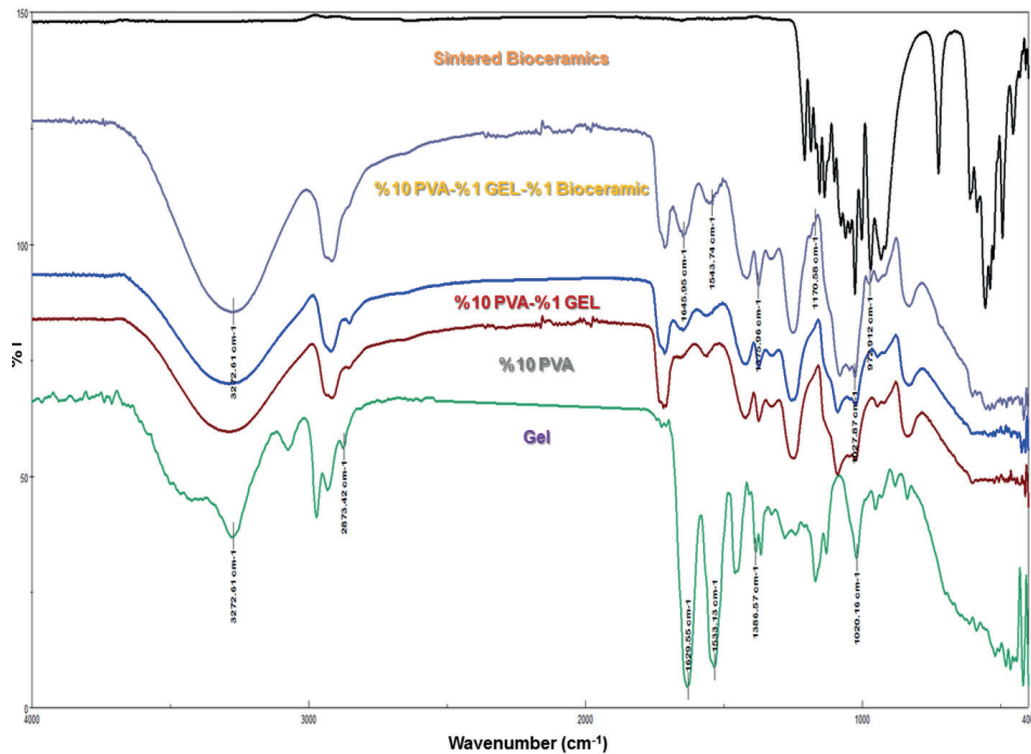


| **Figure 2.** FTIR spectra of bioceramics and scaffold composites.

### **Morphological characterization by FEGSEM analysis**

When examining the FEGSEM morphological images of bioceramic powders synthesized from sea snail shells and sintered at  $850^{\circ}\text{C}$  for 4 hours (Figure 3), particles with various allotropic structures, including spherical, cubic, and needle-like forms, were observed (Buluş, 2017). These diverse particles exhibit high bioresorbability and bioactivity for a bioceramic (Biesuz et al., 2021).

The FEGSEM morphological analysis of the scaffolds (Figure 3) revealed that the fiber diameters of the 10:0 (PVA: GEL) sample ranged between 92 and 205 nm. The incorporation of 1% GEL produced the thinnest fibers observed in the study, with diameters measured between 72 and 142 nm. While the addition of 1% GEL promoted significant fiber thinning. Increasing the GEL content to 3% caused a rise in solution viscosity, leading to thicker fibers with diameters ranging from 145 to 308 nm. Moreover, the incorporation of 1% bioceramic into the 10% PVA/1% GEL composite resulted in nanofiber scaffolds with fiber diameters in the range of 85 to 280 nm. Among all the samples, the 10:1 (PVA: GEL) composite exhibited the thinnest average fiber diameter (Gautam et al., 2021). The mean fiber diameters for each scaffold composition are detailed in Table 3.

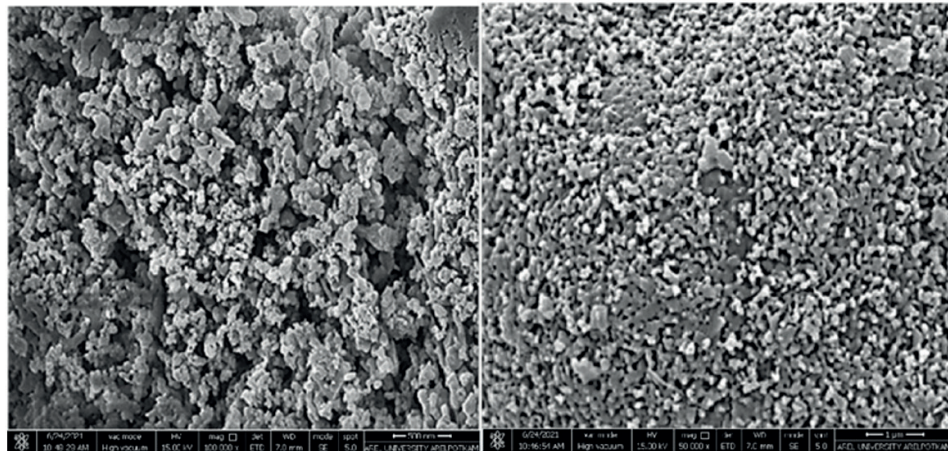


Figure 3. SEM Images of Bioceramic Powders Synthesized from Sea Snail Shells.

These findings underscore the critical role of additive materials in the composite, modulating the morphological properties of nanofiber scaffolds. Such insights are particularly valuable for advancing the design of scaffold materials in biomedical applications, where precise control over fiber dimensions is essential.

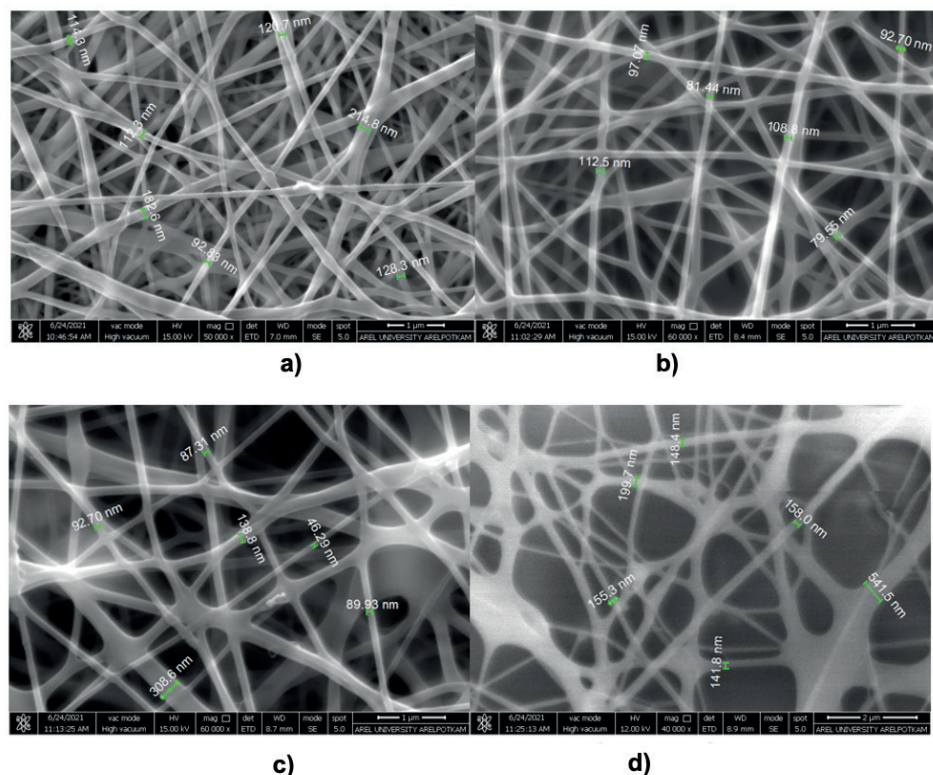


Figure 3. SEM images of tissue scaffolds a) 10:0 (PVA: GEL) b) 10:1 (PVA: GEL) c) 10:3 (PVA: GEL) d) 10:1:1 (PVA: GEL: Bioceramics).

**Table 3.** Mean fiber diameters of tissue scaffolds.

Sample	Mean Fiber Diameter (nm)
10:0 (PVA: GEL)	92-205
10:1 (PVA: GEL)	72-142
10:3 (PVA: GEL)	145-308
10:1:1 (PVA: GEL:Bioceramics)	85-280

### **Mechanical characterization (Tensile test)**

Tensile test results show that the 10:0 (PVA: GEL) sample exhibited a tensile strength of 6.25 MPa, which increased to 7.45 MPa with the addition of 1% GEL. The tensile strength in the 10:3 (PVA: GEL) sample was higher than that of the 10:1 (PVA: GEL) membrane. The gel is a protein-based polymer and has the capacity to form hydrogen bonds. PVA is also a polymer prone to hydrogen bonds. The increase in the gel ratio allows the formation of more hydrogen bonds in the PVA matrix. These bonds are thought to increase the mechanical strength of the nanofiber membrane by strengthening the interactions between the polymer chains (Qiao et al., 2015). Additionally, incorporation of 1% bioceramic into the 10% PVA/1% GEL composite further enhanced the tensile strength of the 10:1:1(PVA: GEL: Bioceramics) scaffolds. The strongest sample in the study was identified as the 10:1:1(PVA: GEL: Bioceramics) composite, achieving a tensile strength value of 8.22 MPa (Table 4).

**Table 4.** Tensile strengths of the composite scaffolds.

Sample	Tensile Strength (MPa)
10:0 (PVA: GEL)	6.25
10:1 (PVA: GEL)	7.45
10:3 (PVA: GEL)	8.01
10:1:1(PVA:GEL:Bioceramics)	8.22

As a result of the homogeneous wrapping of the PVA-GEL nanofibers by the bioceramics, nanofibers with larger surface areas were obtained. This is an indication of the linear increase observed in the tensile strength of the membranes. Moreover, the addition of bioceramic material contributed to the reinforcement of the polymer fibers by integrating into the matrix and enhancing the fiber strength (Hejazi et al., 2021; Şahin,2019; Altan et al., 2024). These findings highlight the synergistic effect of GEL and bioceramic additives in optimizing the mechanical properties of nanofiber scaffolds, making them suitable for applications requiring enhanced structural integrity.

## **Conclusions**

This study successfully synthesized bioceramics from sea snail shells through the chemical precipitation method. Using PVA, GEL, and bioceramic powders, nanofiber-structured tissue scaffolds were fabricated via the electrospinning technique. The methodology employed demonstrated the effective integration of bioceramic components into the polymer matrix, producing a composite material with desirable properties for tissue engineering applications. The results of the study indicate that the synthesized bioceramics, when incorporated into tissue scaffolds, yield a biomaterial with promising



characteristics, including ideal mechanical and structural properties. These scaffolds exhibited suitable porosity and nanofiber morphology, which are critical for mimicking the extracellular matrix and promoting cell adhesion, proliferation, and differentiation. The FTIR and SEM analyzes further confirmed the successful integration of bioceramics into the composite structure, demonstrating their compatibility with the polymer matrix and the maintenance of functional group integrity. The mechanical characterization results revealed that the composite scaffolds provide tensile strength, making them suitable for applications requiring load-bearing capacity, such as in bone and connective tissue regeneration. Moreover, the bioceramic component contributes to bioactivity and biocompatibility, facilitating interactions with surrounding tissues and promoting mineralization and osseointegration. Given these properties, it is anticipated that the composite scaffolds can serve as an interfacial layer in various tissue engineering applications. Their ability to create an environment conducive to cell adhesion and tissue regeneration suggests potential for use in dental applications, particularly for supporting bone and connective tissue formation. Additionally, the rapid biodegradability and bioresorbability of these scaffolds minimize long-term risks, making them a sustainable option for clinical applications. Future studies could focus on in vitro and in vivo assessments to further validate the bioactivity, biocompatibility, and mechanical performance of these scaffolds. Furthermore, exploring the scalability of the fabrication process and its adaptability to other bioceramic-polymer composites could pave the way for broader biomedical applications.

## Acknowledgements

This research was supported by the Polymer Technologies and Composite Materials Research and Development Center (ArelPOTKAM) at Istanbul Arel University, Türkiye.

## Funding

None.

## Conflict of interest

The authors declare no conflict of interest.

## Data availability statement

Data can be obtained from the corresponding author upon a reasonable request.

## Ethics committee approval

Ethics committee approval is not required for this study.

## Authors' contribution statement

The authors acknowledge their contributions to this paper as follows: **Study conception and design:** Y.M.S.; E.B.,; **Data collection:** S.N.S., A.T.; **Analysis and interpretation of results:** S.N.S., A.T., E.B., M.U.F., M.A., Y.M.S.; **Manuscript draft preparation:** S.N.S., A.T., E.B., M.U.F., M.A., Y.M.S. All authors reviewed the results and approved the final version of the manuscript.

## ORCIDs and emails of the authors

Sema Nur Sahin | ORCID 0000-0003-3549-7646 | [semanuursahin@gmail.com](mailto:semanuursahin@gmail.com)

Erdi Bulus | ORCID 0000-0002-2045-2499 | [erdibulus@arel.edu.tr](mailto:erdibulus@arel.edu.tr)

Alper Tezcan | ORCID 0000-0002-4603-9061 | [alpertzcan@arel.edu.tr](mailto:alpertzcan@arel.edu.tr)

Muhammad Umar Farooq | ORCID 0000-0001-8804-9754 | [ufbajwa@yahoo.com](mailto:ufbajwa@yahoo.com)

Marwah Al-garash | [meroalgarash@gmail.com](mailto:meroalgarash@gmail.com)

Yesim Muge Sahin | ORCID 0000-0003-2119-1216 | [ymugesahin@arel.edu.tr](mailto:ymugesahin@arel.edu.tr)

## References

- Altan, D., Özarslan, A. C., Özel, C., Tuzlakoglu, K., Sahin, Y. M., & Yücel, S. (2024). Fabrication of electrospun double layered biomimetic collagen–chitosan polymeric membranes with zinc-doped mesoporous bioactive glass additives. *Polymers*, 16(14), 2066–2084. <https://doi.org/10.3390/polym16142066>
- Aydogdu, M. O., Mutlu, B., Kurt, M., Inan, A. T., Kuruca, S. E., Erdemir, G., Sahin, Y.M., Ekren, N., Oktar, F.N., & Gunduz, O. (2019). Developments of 3D polycaprolactone/beta-tricalcium phosphate/collagen scaffolds for hard tissue engineering. *Journal of the Australian ceramic society*, 55, 849-855. <https://doi.org/10.1007/s41779-018-00299-y>
- Ba Linh, N. T., Lee, K. H., & Lee, B. T. (2013). Functional nanofiber mat of polyvinyl alcohol/gelatin containing nanoparticles of biphasic calcium phosphate for bone regeneration in rat calvaria defects. *Journal of biomedical materials research part A*, 101(8), 2412–2423. <https://doi.org/10.1002/jbm.a.34533>
- Biesuz, M., Galotta, A., Motta, A., Kermani, S., Grasso, J., Vontorová, V., Tyrpekl, M., Vilémová, M., & Sglavo, V. M. (2021). Speedy bioceramics: Rapid densification of tricalcium phosphate by ultrafast high-temperature sintering. *Materials science and engineering: C*, 127, 112246. <https://doi.org/10.1016/j.msec.2021.112246>
- Buluş, E. (2017). *Doğal izole edilmiş biyoseramiklerden elektrospinning yöntemi ile polimerik biyokompozit malzeme eldesi* (Master's thesis, Fen Bilimleri Enstitüsü).
- Bulus, E., Sakarya Bulus, G., & Sahin, Y. M. (2020). Production and characterization of nanotechnological tape for wounds caused by diabetes. *Journal of materials and electronic devices*, 5(1), 20–24.
- Cam, M. E., Cesur, S., Taskin, T., Erdemir, G., Kuruca, D. S., Sahin, Y. M., Kabasakal, L., & Gunduz, O. (2019). Fabrication, characterization and fibroblast proliferative activity of electrospun Achillea lycaonica-loaded nanofibrous mats. *European polymer journal*, 120, 109239. <https://doi.org/10.1016/j.eurpolymj.2019.109239>
- Filippi, M., Born, G., Chaaban, M., & Scherberich, A. (2020). Natural polymeric scaffolds in bone regeneration. *Frontiers in bioengineering and biotechnology*, 8, 474. <https://doi.org/10.3389/fbioe.2020.00474>
- Gautam, S., Sharma, C., Purohit, S. D., Singh, H., Dinda, A. K., Potdar, C. F., Chou, P. D., & Mishra, N. C. (2021). Gelatin-polycaprolactone-nanohydroxyapatite electrospun nanocomposite scaffold for bone tissue engineering. *Materials science and engineering: C*, 119, 111588. <https://doi.org/10.1016/j.msec.2020.111588>
- Gunduz, O., Sahin, Y. M., Agathopoulos, S., Ağaoğulları, H., Gökçe, E. S., Kayali, C., Aktas, B., Ben-Nissan, B., & Oktar, F. N. (2013). Nano calcium phosphate powder production through chemical

- agitation from Atlantic deer cowrie shells (*Cypraea cervus Linnaeus*). *Key engineering materials*, 587, 80–85. <https://doi.org/10.4028/www.scientific.net/KEM.587.80>
- Hernández, G. R., Valdez, H. A., Arango-Ospina, M., Delgado, J. F., Aguilar-Rabiela, A. E., Gorgojo, J. P., Zhang, H., Beltrán, A.M., Boccaccini, A.R., & Sánchez, M. L. (2024). PVA-gelatine based hydrogel loaded with astaxanthin and mesoporous bioactive glass nanoparticles for wound healing. *Journal of drug delivery science and technology*, 101, 106235. <https://doi.org/10.1016/j.jddst.2024.106235>
- Hejazi, F., Bagheri-Khoulenjani, S., Olov, D., Zeini, A., Solouk, A., & Mirzadeh, H. (2021). Fabrication of nanocomposite/nanofibrous functionally graded biomimetic scaffolds for osteochondral tissue regeneration. *Journal of biomedical materials research part A*, 109(9), 1657–1669. <https://doi.org/10.1002/jbm.a.37161>
- Heydary, H. A., Karamian, E., Poorazizi, E., Heydaripour, J., & Khandan, A. (2015). Electrospun of polymer/bioceramic nanocomposite as a new soft tissue for biomedical applications. *Journal of asian ceramic societies*, 3(4), 417–425. <https://doi.org/10.1016/j.jascer.2015.09.003>
- Hong, J., Yeo, M., Yang, G. H., & Kim, G. H. (2019). Cell-electrospinning and its application for tissue engineering. *International journal of molecular sciences*, 20(24), 6208. <https://doi.org/10.3390/ijms20246208>
- Hoque, M. E., Sakinah, N., Chuan, Y. L., & Ansari, M. N. M. (2014). Synthesis and characterization of hydroxyapatite bioceramic. *International journal of scientific engineering and technology*, 3(5), 458–462.
- Howard, D., Buttery, L. D., Shakesheff, K. M., & Roberts, S. J. (2008). Tissue engineering: Strategies, stem cells and scaffolds. *Journal of anatomy*, 213(1), 66–72. <https://doi.org/10.1111/j.1469-7580.2008.00878.x>
- Jazayeri, H. E., Lee, S.-M., Kuhn, L., Fahimipour, F., Tahriri, M., & Tayebi, L. (2020). Polymeric scaffolds for dental pulp tissue engineering: A review. *Dental materials*, 36(2), e1–e10. <https://doi.org/10.1016/j.dental.2019.11.005>
- Keçeciler-Emir, C., Başaran-Elalmiş, Y. M., Şahin, Y., Buluş, E., & Yücel, S. (2023). Fabrication and characterization of chlorhexidine gluconate loaded poly (vinyl alcohol)/45S5 nano-bioactive glass nanofibrous membrane for guided tissue regeneration applications. *Biopolymers*, 114(10), e23562. <https://doi.org/10.1002/bip.23562>
- Linh, N. T., Min, Y. K., Song, H. Y., & Lee, B. T. (2010). Fabrication of polyvinyl alcohol/gelatin nanofiber composites and evaluation of their material properties. *Journal of biomedical materials research part B: applied biomaterials*, 95(1), 184–191. <https://doi.org/10.1002/jbm.b.31701>
- Mazumder, S., Nayak, A. K., Ara, T. J., & Hasnain, M. S. (2019). Hydroxyapatite composites for dentistry. In *Applications of nanocomposite materials in dentistry* (pp. 123–143). <https://doi.org/10.1016/B978-0-12-813742-0.00007-9>
- Perez-Puyana, V., Jiménez-Rosado, M., Romero, A., & Guerrero, A. (2018). Development of PVA/gelatin nanofibrous scaffolds for tissue engineering via electrospinning. *Materials research express*, 5(3), 035401. <https://doi.org/10.1088/2053-1591/aab164>
- Razzaq, A., Khan, Z. U., Saeed, A., Shah, K. A., Khan, N. U., Menaa, B., Iqbal, H., & Menaa, F.

- (2021). Development of cephradine-loaded gelatin/polyvinyl alcohol electrospun nanofibers for effective diabetic wound healing: *In vitro* and *in vivo* assessments. *Pharmaceutics*, 13(3), 349. <https://doi.org/10.3390/pharmaceutics13030349>
- Sadeghi, A., Pezeshki-Modaress, M., & Zandi, M. (2018). Electrospun polyvinyl alcohol/gelatin/chondroitin sulfate nanofibrous scaffold: Fabrication and *in vitro* evaluation. *International Journal of biological macromolecules*, 114, 1248–1256. <https://doi.org/10.1016/j.ijbiomac.2018.04.002>
- Sahin, Y. M. (2019). Natural nanohydroxyapatite synthesis via ultrasonication from *Donax trunculus* bivalve sea shells and production of its electrospun nanobiocomposite. *Acta physica polonica A*, 135(5), 1093–1096. <https://doi.org/10.12693/APhysPolA.135.1093>
- Sahin, Y. M., Orman, Z., & Yucel, S. (2018). *In vitro* studies of  $\alpha$ -TCP and  $\beta$ -TCP produced from *Clinocardium ciliatum* seashells. *Journal of the Australian ceramic society*, 56, 477–488. <https://doi.org/10.1007/s41779-019-00355-1>
- Şahin, Y. M., Orman, Z., & Yücel, S. (2018). A simple chemical method for conversion of *Turritella terebra* sea snail into nanobioceramics. *Journal of ceramic processing research*, 19(6), 492–498. ISSN: 1229-9162
- Santhosh, S., & Balasivanandha Prabu, S. (2013). Thermal stability of nano hydroxyapatite synthesized from sea shells through wet chemical synthesis. *Materials letters*, 97, 121–124. <https://doi.org/10.1016/j.matlet.2013.01.081>
- Sengor, M., Ozgun, A., Corapcioglu, G., Ipekoglu, M., Garipcan, B., Ersoy, N., & Altintas, S. (2018). Core-shell PVA/gelatin nanofibrous scaffolds using co-solvent, aqueous electrospinning: Toward a green approach. *Journal of applied polymer science*, 135(32), 46582. <https://doi.org/10.1002/app.46582>
- Song, W., Markel, D. C., Wang, T., Shi, G., Mao, T., & Ren, W. (2012). Electrospun polyvinyl alcohol–collagen–hydroxyapatite nanofibers: A biomimetic extracellular matrix for osteoblastic cells. *Nanotechnology*, 23(11), 115101. <https://doi.org/10.1088/0957-4484/23/11/115101>
- Tüzün, E. (2023). Synthesis of novel antioxidant carboxymethylcellulose nanocomposites for Cu–Ni–Mo-based steel foams. *Cellulose*, 30(14), 8753–8768. <https://doi.org/10.1007/s10570-023-05436-w>
- Qiao, K., Zheng, Y., Guo, S., Tan, J., Chen, X., Li, J., Xu, D., & Wang, J. (2015). Hydrophilic nanofiber of bacterial cellulose guided the changes in the micro-structure and mechanical properties of nf-BC/PVA composites hydrogels. *Composites science and technology*, 118, 47–54. <https://doi.org/10.1016/j.compscitech.2015.08.004>
- Xie, W., Fu, X., Tang, F., Mo, Y., Cheng, J., Wang, H., & Chen, X. (2019). Dose-dependent modulation effects of bioactive glass particles on macrophages and diabetic wound healing. *Journal of materials chemistry B*, 7(6), 940–952. <https://doi.org/10.1039/C8TB02938E>
- Yelten-Yilmaz, A., & Yilmaz, S. (2010). Wet chemical precipitation synthesis of hydroxyapatite (HA) powders. *Ceramics international*, 44(8), 9703–9710. <https://doi.org/10.1016/j.ceramint.2018.02.201>
- Zhang, H., Xiong, Y., Dong, L., & Li, X. (2021). Development of hierarchical porous bioceramic scaffolds with controlled micro/nano surface topography for accelerating bone regeneration.

*Materials science and engineering: C*, 130, 112437. <https://doi.org/10.1016/j.msec.2021.112437>

Zou, Y., Zhang, L., Yang, F., Zhu, M., Ding, F., Lin, Z., Wang, Z., & Li, Y. (2018). 'Click' chemistry in polymeric scaffolds: Bioactive materials for tissue engineering. *Journal of controlled release*, 273, 160–179. <https://doi.org/10.1016/j.jconrel.2018.01.023>